J. Cent. South Univ. (2014) 21: 272−286
DOI: 10.1007/s11771-014-1938-z

Springer

Objective measurement for image defogging algorithms

GUO Fan(郭璠)[1, 2], TANG Jin(唐瑾)[1], CAI Zi-xing(蔡自兴)[1]

1. School of Information Science and Engineering, Central South University, Changsha 410083, China;
2. Hunan Engineering Laboratory for Advanced Control and Intelligent Automation (Central South University), Changsha 410083, China

Abstract: Since there is lack of methodology to assess the performance of defogging algorithm and the existing assessment methods have some limitations, three new methods for assessing the defogging algorithm were proposed. One was using synthetic foggy image simulated by image degradation model to assess the defogging algorithm in full-reference way. In this method, the absolute difference was computed between the synthetic image with and without fog. The other two were computing the fog density of gray level image or constructing assessment system of color image from human visual perception to assess the defogging algorithm in no-reference way. For these methods, an assessment function was defined to evaluate algorithm performance from the function value. Using the defogging algorithm comparison, the experimental results demonstrate the effectiveness and reliability of the proposed methods.

Key words: image defogging algorithm; image assessment; simulated foggy image; fog density; human visual perception

1 Introduction

Due to the adverse weather conditions like the presence fog or heavy rain, digital images are easily subjected to a wide variety of disturbance during acquisition, which may reduce visual effect and affect post-processing of the image. Because of the importance of the defogging algorithm, much work has been done [1−3]. Subjective evaluation, as the main method to assess the efficiency and effectiveness of the enhancement algorithm at present is easily plagued by observer's subjective feeling, which makes the evaluation results unreliable. Specifically, the reasons for the difficulties of defogging effect assessment are: 1) No ideal image can be taken as assessment reference image. The assessment for defogging effect is different from the image quality or image restoration assessment, for the no-fog day reference image that has completely the same scene with foggy image is usually very hard to get; 2) The evaluation criteria for defogging effect should be consistent with human visual perception. However, the human visual perception itself is not a deterministic process. Therefore, it is hard to determine the most important factors that affect visual decision and to design the corresponding assessment indicators; 3) The traditional image quality assessment indexes, such as mean square error (MSE), entropy of information, peak signal to noise ratio (PSNR), are often adopted for defogging algorithm assessment. However, they usually get the inconsistent results. Thus, it is very important to research on the objective assessment method of image defogging algorithm. Recently, objective image quality evaluation approaches can be classified into three categories: full-reference [4−5], reduced-reference [6] and no-reference or "blind" quality assessment approach [7], depending on the requirement for reference image. For the image defogging algorithm, the objective assessment method can be classified into two categories: 1) assessing from the image contrast. A typical contrast-based enhancement algorithm is proposed by HAUTIERE et al [8]. The method computes the ratio between gradient of the visible edges between the image before and after contrast restoration. In this way, three indicators of contrast measurement are provided based on the concept of visibility level. 2) Assessing from both image contrast and image color [9]. The extent of contrast enhancement from global and local contrast of defogging image is measured. Meanwhile, the hue polar histogram, principal component analysis of RGB image and histogram similarity are used to assess the image color quality from hue reproduction capacity, color

Foundation item: Projects(91220301, 61175064, 61273314) supported by the National Natural Science Foundation of China; Project(126648) supported by the Postdoctoral Science Foundation of Central South University, China; Project(2012170301) supported by the New Teacher Fund for School of Information Science and Engineering, Central South University, China
Received date: 2012−07−30; **Accepted date:** 2012−12−07
Corresponding author: TANG Jin, Professor, PhD; Tel: +86−18627570085; E-mail: tjin@csu.edu.cn

reproduction capacity and naturalness. Canny edge detector and bright channel are used to detect the intensity of effective edge, and also the histogram similarity is utilized to denote the color performance of the defogging image [10]. The notions of detail restoration ratio and color restoration ratio are proposed [11], with which the effect of different defogging algorithms can be also evaluated objectively from the image contrast and color.

In this work, the limitations of the existing method were enumerated, and then three assessment methods for image defogging algorithm by using the full-reference and no-reference way were proposed. One is using synthetic foggy image simulated by image degradation model, and the other two are computing the fog density of gray level image or constructing assessment system of color image from human visual perception. The former is a full-reference method which needs images of the same scene with and without fog. However, obtaining such kind of pairs of images is extremely difficult in practice since it requires checking that the illumination conditions are the same into the scene. Thus, a set of synthetic images with and without fog is built up by using virtual reality technique for the defogging effect evaluation. The latter two are no-reference methods based on the fog density or human visual perception. Fog veil and dark channel are used in the fog density method to estimate fog density, while the evaluation function method combines three components, contrast, naturalness and colorfulness to yield an overall defogging result measure. Meanwhile, by doing statistics to the series of image sequences from dense fog to over enhancement, the overall variation trends of the three components are analyzed to construct a comprehensive evaluation function for assessing the image defogging algorithm.

The three assessment methods have fundamental differences in solutions and all have pluses and minuses, so which method should be chosen depends on the assessment object and the goal in real situation. Specifically, if we want to evaluate the defogging performance of the algorithms on the whole, the synthetic image method should be adopted. While for the comparison with existing defogging algorithms for a given foggy image, the fog density method or evaluation function method can be used. Compared with other works, this proposed assessment methods have the following advantages: 1) Ideal no-fog reference images are generated for the assessment method based on synthetic image, which provides a new solution to the problem of the defogging algorithm assessment, and 2) The most sensitive factors for subjective assessment are determined from the perspective of fog density or human visual perception, which ensures that the assessment results are consistent with human visual perception.

2 Defogging algorithm assessment based on visibility edges

So far, there have been many works to remove fog from image, but only few researches focus on the quantitative measure of defogging effect. In Refs. [2, 8], a method for contrast enhancement assessment was proposed based on the concept of visibility level, which is commonly used.

2.1 Theoretical foundation

In the International Commission on Illumination (CIE) Report 19.2, BLACKWELL et al [12] introduced a descriptive term visibility level L_v. L_v is obtained by the ratio of the actual luminance difference of the target display to its threshold value, which is defined as [12]

$$L_v = \frac{\Delta L_{\text{actual}}}{\Delta L_{\text{threshold}}} \tag{1}$$

where ΔL_{actual} can be estimated by measuring the luminance of the target and its background, and ADRIAN's empirical target visibility model [13] can be used to compute the luminance difference threshold $\Delta L_{\text{threshold}}$. However, for a complex image which contains several objects on a non-uniform background, to calculate the value of $\Delta L_{\text{threshold}}$ is still a challenging task. Fortunately, to solely assess the performance of a contrast restoration method, the approach described in Ref. [8] is much easier. It is proposed to compute the following coefficient r as

$$r = \frac{L_{vr}}{L_{v0}} = \frac{\Delta I_r}{\Delta I_0} \tag{2}$$

where ΔL_{vr} and L_{v0} denote the visibility level of the considered object in restored image and the original image, respectively. ΔI_r and ΔI_0 denote the gradient in the restored image and original image, respectively. Consequently, the computation of r enables to compute the gain of visibility level produced by a defogging algorithm, which is measured by the gradient of each pixel belonging to a visible edge in the restored and original image.

2.2 Assessment index

Defogging effect assessment based on visibility edges [8] obtains contrast map with logarithmic image processing (LIP) model and the definition of the meteorological visibility distance proposed by CIE. Figure 1 shows the contrast map for some results of

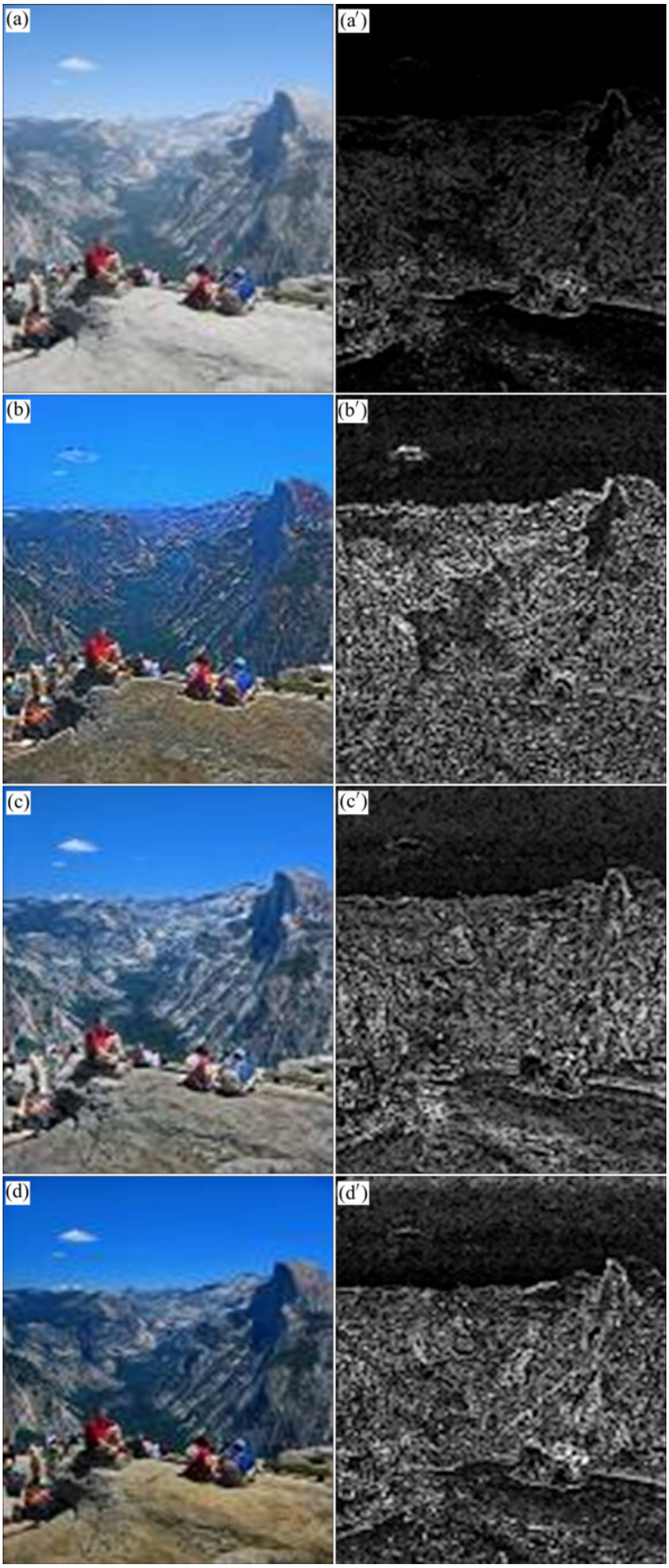

Fig. 1 Defogging results ((a), (b), (c)) and corresponding contrast map ((a′), (b′), (c′)): (a), (a′) Original image; (b), (b′) TAN's result; (c), (c′) TAREL's result; (d), (d′) HE's result

defogging algorithms. Three descriptors including the rate e of edges newly visible after restoration, the mean $\bar{r}$ over these edges of the ratio of the gradient norms after and before defogging, and the percentage of pixels σ which becomes saturated (black or white) after defogging but not before, are computed to objectively assess defogging effect from different angles:

$$e=\frac{n_{\mathrm{r}}-n_0}{n_0} \tag{3}$$

$$\bar{r}=\exp\left[\frac{1}{n_r}\sum_{P_i\in S_r}\log r_i\right] \tag{4}$$

$$\sigma=\frac{n_{\mathrm{s}}}{w\cdot h} \tag{5}$$

where n_0 and n_{r} denote respectively the cardinal numbers of the set of visible edges in the original image I_0 and in the defogging image I_{r}. S_r is the set of visible edge in I_{r}. P_i denotes the pixels that belong to the visible edge of image I_{r}, r_i is the ratio of the Sobel gradient at P_i in the image I_{r} and I_0. n_{s} is the number of pixels which becomes saturated (black or white). w and h denote respectively the width and the height of the image.

For each defogging algorithm, the main aim is to increase the contrast without saturating and thus losing some visual information. Hence, the quality of the defogging can be expressed by the three descriptors, and good results are described by high values of e and $\bar{r}$ and low values of σ. Table 1 presents the three descriptors computed for the defogging images in Fig. 1. Note that the value of e may be negative. This could happen when the original image is enhanced over certain extent. Although there are more visibility pixels, these pixels connect together, which makes the visibility edges become less.

Table 1 Three descriptors computed for three compared methods in Fig. 1

Reference	e	$\bar{r}$	σ
[1]	−0.08	2.08	0.005
[2]	−0.008	2.01	0
[3]	0.06	1.42	0.002

2.3 Limitation

2.3.1 Effect definition problem

The most fundamental problem with the approach in Ref. [8] is the definition of defogging effect. In particular, it is not always true that higher values of e or $\bar{r}$, and lower values of σ correspond to a better defogging results. An obvious example would be the over enhancement which may be clearly visible but not so objectionable. From Table 1, it is deduced that TAN's algorithm is the best because of the highest $\bar{r}$. However, the algorithm probably increases the contrast so strong that the image may have halos near some edges and the color after defogging also seems unnatural.

2.3.2 Inconsistency problem

When one chooses to use one of the descriptors to assess the defogging effect, it is implicitly assumed that the best defogging algorithms should be picked out by any descriptor. In a word, the best algorithm should have the highest e, $\bar{r}$ and lowest σ at the same time. Empirically, however, this is not the case for the state of art algorithms as shown in Table 1. In fact, the best algorithm may be a trade-off among these descriptors. Thus, it remains to be seen how much these descriptors can assess the performance of the current defogging algorithms.

3 Defogging algorithm assessment based on synthetic image

For objective assessment method, full-reference way is the most reliable. However, there is no easy way to have a reference image. Thus, a synthetic image database with and without fog was built up. The database comprised 54 synthetic images of 18 urban road scenes. Each image without fog was associated with a foggy image and a transmission map. Fog was added on each image according to image degradation model, and the size of each image was 640×480. These scenes were used to test defogging algorithms intensively in an objective way.

3.1 Generation of synthetic image

The generation of synthetic image made full use of the depth information to let the distant objects in the scene gradually disappear in the fog. Therefore, the generated fog had very natural visual effect. The image degradation model [14] that describes the degradation process and mechanism of the foggy image is the theoretic foundation of the assessment method. The formation of an image degradation model is as follows:

$$I(x)=J(x)\mathrm{e}^{-\beta d(X)}+A(1-\mathrm{e}^{-\beta d(X)}) \tag{6}$$

where x is the scene point corresponding to pixel X=(x, y), A is the atmospheric light value, which can be obtained by using the defogging algorithms proposed by HE et al [3] and YU et al [15], d(X) is the distance along the real-word ray corresponding to the pixel X, β is the atmospheric attenuation coefficient due to the light scattering. According to the radiative transport Equation proposed by ROSSUM and NIEUWENHUIZN [16], let $t(X)=\mathrm{e}^{-\beta d(X)}$, and t(X) is the transmission map describing the portion of light that is not scattered and reaches the camera. Considering that the distribution of fog usually changes with the image depth in real situation, the parameter λ was introduced to simulate this type of fog. Specifically, a denser medium can be simulated by multiplying the attenuation coefficient β by a factor of λ. This was achieved by applying the following simple power law transformation of the transmission values as

$$t'(X)=\mathrm{e}^{-\lambda\beta d(X)}=(\mathrm{e}^{-\beta d(X)})^{\lambda}=t(X)^{\lambda} \tag{7}$$

Note that the final fog effect obtained by the transformed transmission map $t'(X)$ mainly depends on the value of parameter λ. Figure 2 shows the simulated foggy images with different λ.

3.2 Application example

In order to validate the effectiveness of the defogging algorithm assessment based on synthetic image, each defogging algorithm on the synthetic fog was applied. HE's algorithm and TAREL's algorithm were used. The result of a group of synthetic foggy images is presented in Fig. 3. The increase of the clearness for the farther objects is that some object barely visible in synthetic foggy image appears clearly in defogging images. A first visual analysis confirms that the enhancement with HE's method allows to keep the good properties of the preservation of image detail and object outline, while the results of TAREL's method show a tendency to have halo artifacts. Therefore, HE's algorithms perform better compared to TAREL's algorithm for the synthetic foggy images, as shown in Fig. 3.

The quantified comparison consisted simply in computing the absolute difference (AD) between the image without fog and the image obtained after fog removal. The results show that the averaged AD values over 18 images are 47.21 for no defogging operation, 35.07 for TAREL's algorithm, and 31.94 for HE's algorithm. One can notice that the AD value of HE's algorithm is smaller, so the algorithm has better defogging effect since its defogging image is more close to the original image without fog. This confirms our observation in Fig. 3.

The evaluation results will be inconsistent when using the assessment method based on visibility edges. The TAREL's results of three indicators in Fig. 3 are 1.09, 5.07 and 0.73, while those of HE's method are 0.98, 2.03 and 0, respectively. One can see that HE's algorithm has smaller σ value, which means that its defogging effect is better. However, the opposite conclusion will be drawn when using e and $\bar{r}$ to assess. Experimental results show that our proposed synthetic image method has no such problem.

4 Defogging algorithm assessment based on fog density

The synthetic image method assessed the image defogging effect by using the simulated images of the

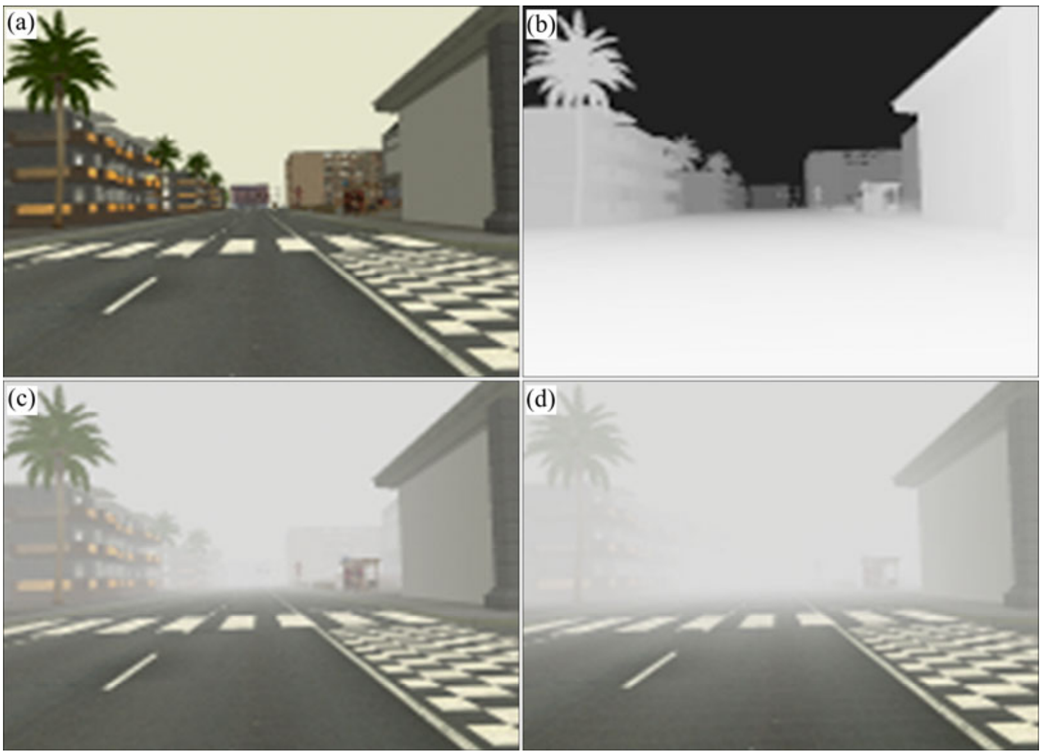

Fig. 2 Synthetic foggy images with different λ by using transmission map: (a) Original image; (b) Transmission map; (c) λ=3; (d) λ=8

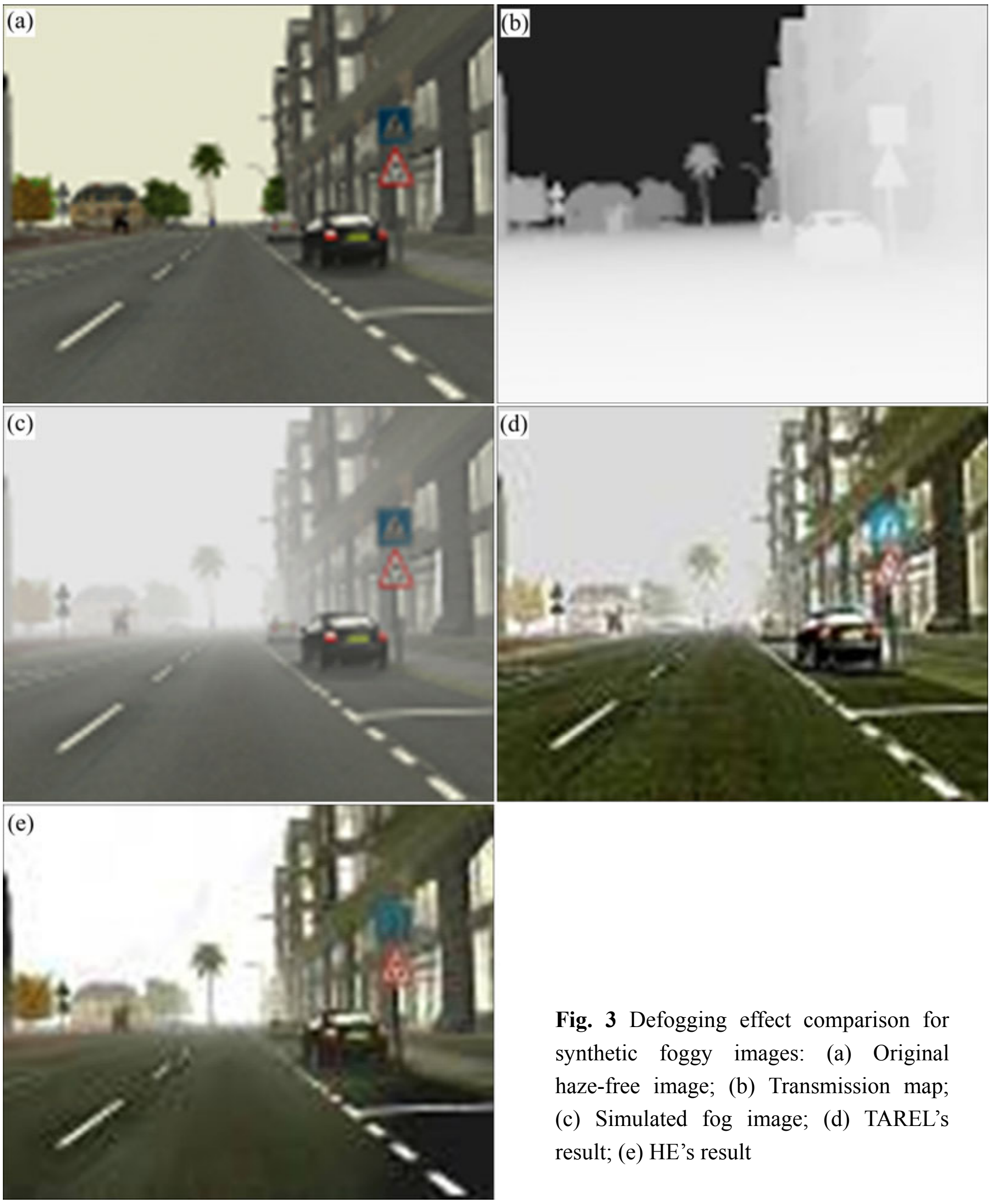

Fig. 3 Defogging effect comparison for synthetic foggy images: (a) Original haze-free image; (b) Transmission map; (c) Simulated fog image; (d) TAREL's result; (e) HE's result

same scene with and without fog in full-reference way. However, there is no easy way to have the reference image in real situation. Thus, no-reference way should be also studied here. Since the fog density is one of the most prominent features for the gray level fog-degraded image, an assessment method is proposed based on the fog density in this section.

4.1 Indicator of fog density method

How to effectively measure fog density is the most important issue for this method. Here, the dark channel and the fog veil are mainly focused, so the density of fog can be defined as

$$f=\sum_{\Omega\in I} D_{c\Omega}(p)V_{\Omega}(p)/HW \tag{8}$$

where, for an image I, D_c is its dark channel computed by using HE's method [3], V is the estimated fog veil for the image, H and W denote respectively the height and the width of the image. The accumulation of the responding each pixel represents the density of fog in the scene.

For the fog veil computation, this process was carried out from R, G, B three color channels of the input image, separately. Define $F(x, y)$ to be Gaussian filter, which is a typical low-pass smoothing function. Firstly, the input image was convoluted with the smoothing function. Then, the fog veil was generated by the mean of $\hat{L}(x,y)$. For a scene with denser fog, the color of fog veil seems correspondingly lighter. The computation process of fog veil can be expressed as follows:

$$\hat{L}(x,y)=I(x,y)\cdot F(x,y) \tag{9}$$

$$\boldsymbol{v}(x,y)=\frac{1}{HW}\sum_{x=1}^{H}\sum_{y=1}^{W}\hat{L}(x,y) \tag{10}$$

An illustrative example of dark channel and fog veil is shown in Fig. 4. One can notice that the bigger values of dark channel D_c and fog veil V lead to denser fog. Thus, we can use the indicator f to make quantitative evaluation of different defogging methods. A smaller value of indicator f implies that the restored image has less fog density, thereby better validating the defogging effect of the algorithms.

4.2 Application example

Some representative defogging algorithms were compared, such as TAN's, TAREL's and HE's method with our proposed indicator. The reason why we chose these algorithms was that they illustrated certain aspects of defogging algorithms. For TAN's method [1], although it can significantly improve image contrast, the results tend to have larger saturation values. It is hoped that these factors can be reflected by our indicator. The reasons for choosing TAREL's method [2] and HE's method [3] were that the former is one of the fastest defogging algorithms at present, and the latter is recognized as one of the most effective ways to remove fog.

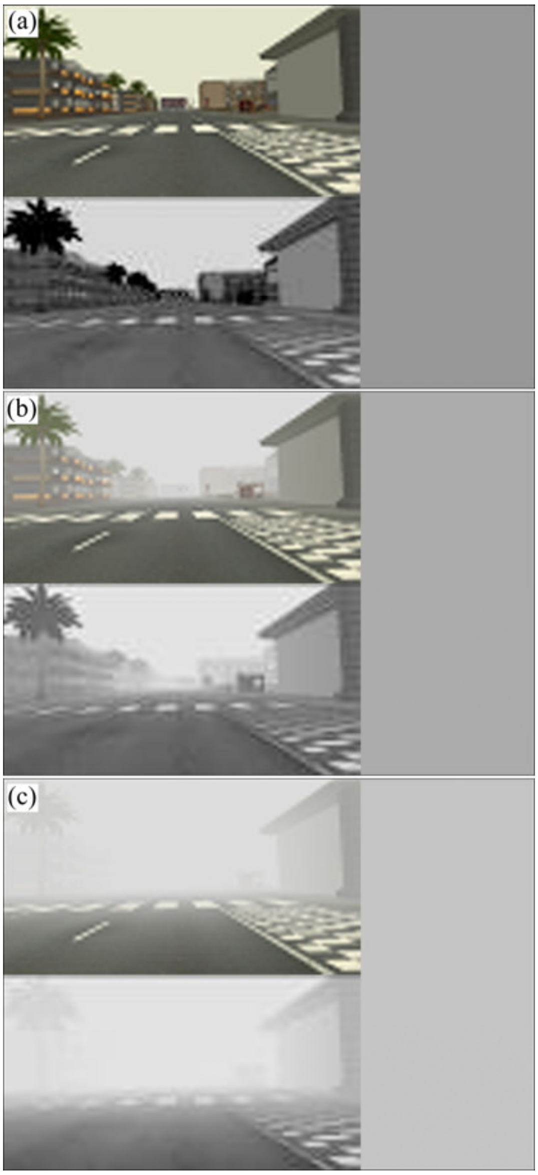

Fig. 4 Input (top), dark channel (bottom) and estimated fog veil images with different fog density: (a) No-fog; (b) Haze; (c) Dense fog

Figures 5−8 show some example images by different defogging algorithms, including both color images and gray level image. The assessment results for these figures with the indicator are listed in Table 2. Clearly, the values of fog density are much reduced after defogging, which proves the validity of all these fog removal algorithms and visual restoration of the defogging images. From Table 2, the three algorithms can be ordered in increasing order with respect to fog density for color images as: TAN, HE and TAREL. However, although TAN's method can greatly eliminate the influence of fog from the perspective of fog density, its visual effect for color images is worse than the other two algorithms due to the color distortion. For TAREL's method and HE's method, depending on image, either algorithm could outperform the other from the perspective of human visual perception. For example, the images produced by TAREL, as shown in Figs. 5(c) and 6(c), are more pleasing than HE's results. In Fig. 7, the images generated by HE's method may have better defogging effect than TAREL's method. We can see that the traffic sign is better restored with realistic colors. Figure 8(a) shows a gray level image. One can notice that HE's result seems more natural, compared to TAREL's and TAN's results. This can also be testified by our proposed indicator in Table 2. Therefore, from the viewpoint of visual effects, the best defogging images are picked out: Figs. 5(c), 6(c), 7(d) and 8(d). Notice that the indicator result for gray level image is consistent with human visual perception, while that is not true for color images. The reason is that we convert the fog veil into gray level image when computing the indicator f, so the color information of the image is lost in that step.

5 Defogging algorithm assessment based on human visual perception

The fog density assessment method is proposed specially for gray level images, so here we constructed a comprehensive measure system from human visual

Fig. 5 Defogging effect comparison for real scene images (1): (a) Haze image; (b) TAN's result; (c) TAREL's result; (d) HE's result

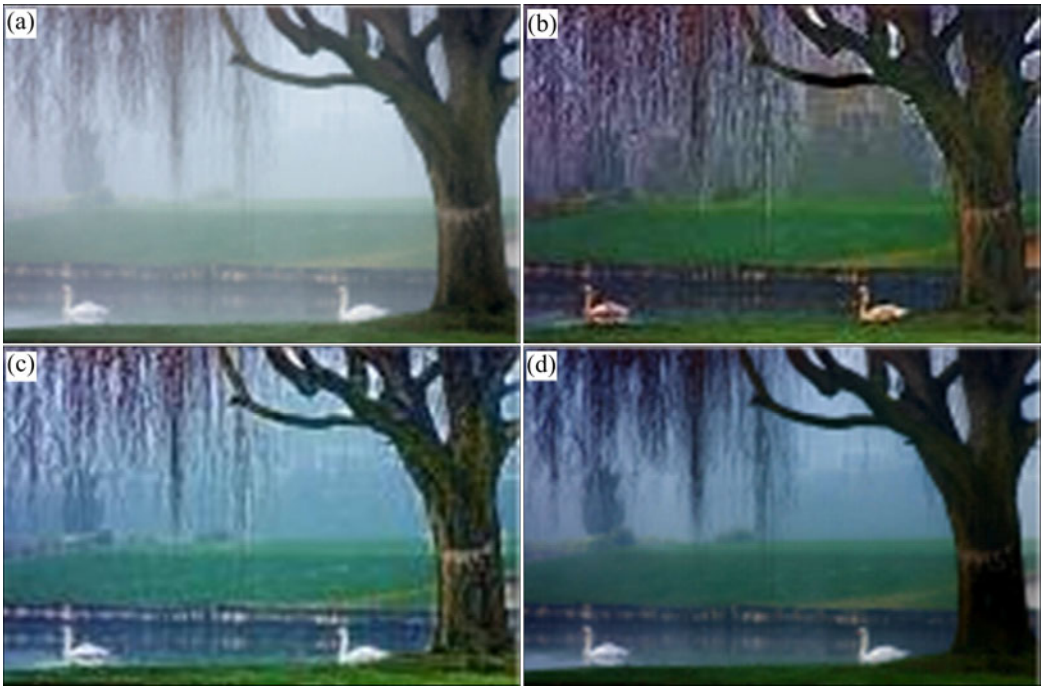

Fig. 6 Defogging effect comparison for real scene images (2): (a) Haze image; (b) TAN's result; (c) TAREL's result; (d) HE's result

perception to handle color images with no need for reference image. For the existing assessment method [8], three descriptors are all based on the contrast map, so the quality of the contrast restoration by the defogging algorithms can be well measured. However, human visual system is highly adapted not only to the contrast, but also to the color quality. Thus, building a comprehensive defogging effect measure system from human visual perception is necessary. In Ref. [17], a model for optimal color image reproduction of natural images was introduced based on the assumption that color quality of natural images was constrained by perceived naturalness and colorfulness of these images. Therefore, two main factors were also considered here: naturalness and colorfulness. These three components, contrast, naturalness, colorfulness, were combined to yield an overall defogging result measure, which is the contrast−naturalness−colorfulness (CNC) index.

Fig. 7 Defogging effect comparison for real scene images (3): (a) Haze image; (b) TAN's result; (c) TAREL's result; (d) HE's result

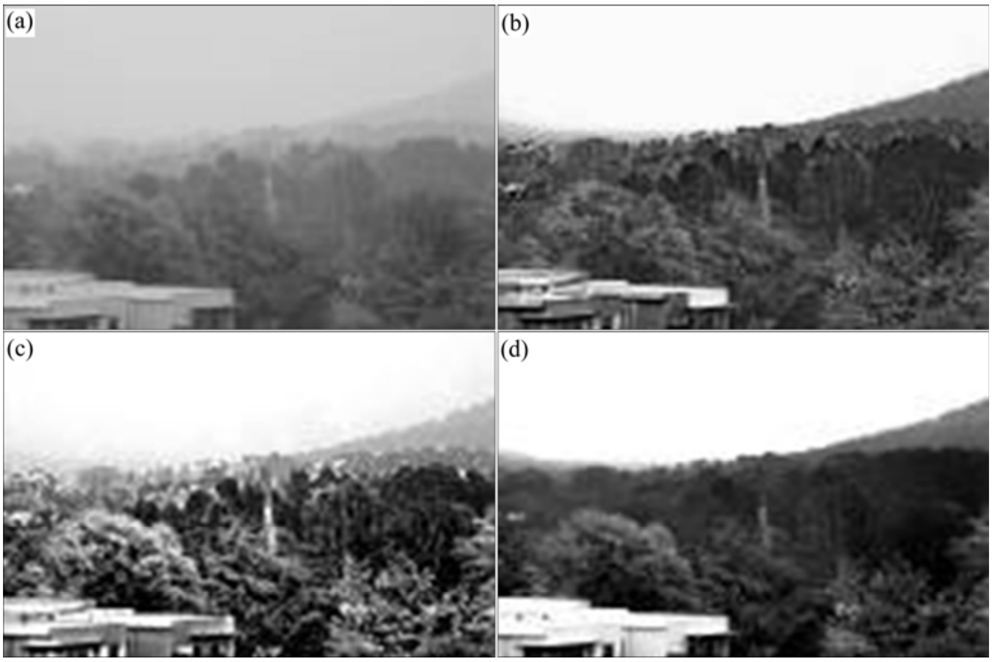

Fig. 8 Defogging effect comparison for real scene images (4): (a) Haze image; (b) TAN's result; (c) TAREL's result; (d) HE's result

Table 2 Comparison of defogging algorithms with indicator based on fog density

Method	Fig. 5 (600×432)		Fig. 6 (835×557)		Fig. 7 (600×400)		Fig. 8 (660×402)	
	v	*f*	*v*	*f*	*v*	*f*	*v*	*f*
Nothing	0.5066	0.0586	0.5598	0.0661	0.6580	0.0915	0.5849	0.0830
TAN [1]	0.2975	0.0143	0.2776	0.0073	0.3242	0.0093	0.5423	0.0646
TAREL and HAUTIERE [2]	0.3688	0.0205	0.4167	0.0189	0.5584	0.0507	0.4641	0.0483
HE et al [3]	0.2303	0.0095	0.3154	0.0137	0.3570	0.0101	0.3821	0.0341

5.1 Framework and components of CNC index

The system diagram of the proposed defogging effect assessment system is shown in Fig. 9. Suppose x is the original foggy image which has unpleasing visual effect, and y is the defogging image, then the CNC measure can serve as a quantitative measurement of the

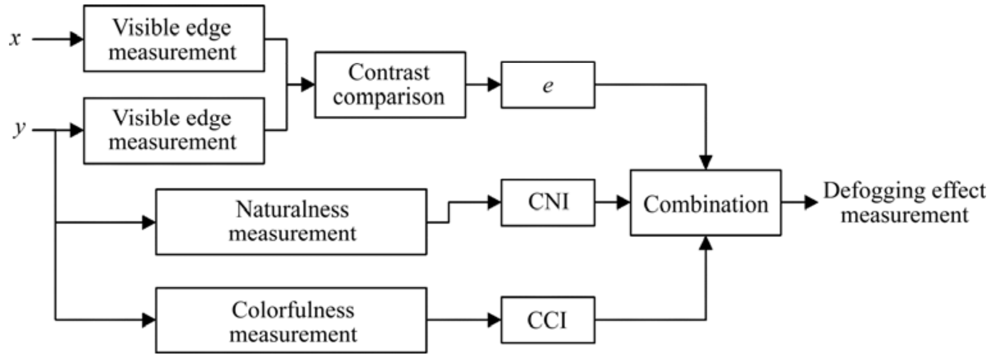

Fig. 9 Diagram of CNC measurement system

defogging effect of *y*. Specifically, the measure system first combined the visible edges of *x* and *y* to compute the contrast measurement index *e*. Then, the image naturalness index CNI and colorfulness index CCI are computed. Finally, the comprehensive function with these three indexes is constructed, and the image defogging effect is assessed by using the function.

The system evaluated the defogging effect from the quality of image contrast and color, and separated the task of defogging effect measurement into three components: contrast, naturalness and colorfulness.

5.1.1 Measurement index for image contrast

According to the definition of visibility distance [12], the visible edge is the reflection of local contrast, so the contrast can be well measured by the number of visible edges in the images. From Eq. (3), one can notice that the value of *e* may be negative when $n_r<n_0$, which means that the number of visible edges after defogging becomes less. Thus, in order to make the descriptor $e\geq0$, for the original image *x* and defogging image *y*, it is defined

$$e(x,y)=\frac{n(y)}{n(x)} \tag{11}$$

where $n(x)$ and $n(y)$ denote respectively the cardinal numbers of the set of visible edges in *x* and *y*.

5.1.2 Measurement index for image naturalness

Naturalness is the degree of correspondence between human perception and reality world, which is described by color naturalness index (CNI) [17−18]. The index is used to measure the defogging image *y*. The bigger the value of CNI is, the more natural the color image is. To ensure the fairness and objectivity of the evaluation, the defogging process uses the criteria of image segmentation and classification proposed in Ref. [18].

5.1.3 Measurement index for image colorfulness

Colorfulness presents the color vividness degree, which is described by CCI [17−18]. The index is also used for measuring the defogging image *y*. When CCI is in certain range, the color of image is suitable for human. CCI is related to image content, and mainly used for measuring the image colorfulness of the same scene in different defogging effects.

In order to analyze these three indexes, the simulated foggy image is created from dense fog, fog, haze, haze-free to over enhancement by gradually adjusting related algorithm parameters for 50 test images. By doing statistics to the series of image sequences from dense fog to over enhancement, the overall variation trend of these three indexes is obtained, as illustrated in Fig. 10.

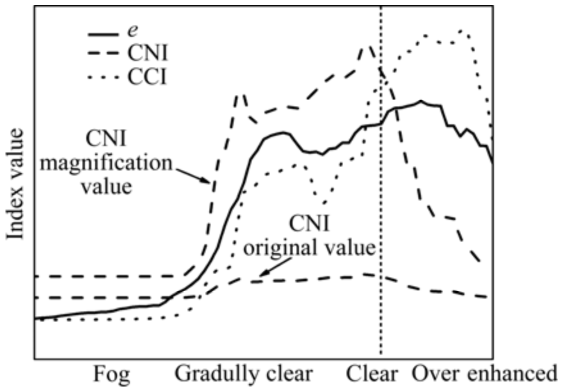

Fig. 10 Overall variation trend of indexes in CNC system

In Fig. 10, solid curve represents the variation trend of contrast measurement index *e*, dotted curves and dashed curves represent that of CCI and CNI, respectively. The best defogging effect position is shown in black dotted line. Compared with the change of *e* and CCI, the value change of CNI is too small. Thus, the value is enlarged artificially, so the relationship among the indexes can be shown intuitively in the same coordinate system. From Fig. 10, it is seen that during the process of gradual clearness, *e* and CCI are ascending at fluctuations. When the image is over-enhanced, the two values still increase until the curve increases to a certain degree, and then they begin to descend rapidly, which means that *e* and CCI achieve the best defogging effect before the peak. Here, the fluctuation of *e* curve is because the visibility pixels construct the edges connecting together, which causes the number of visibility edges in the defogging image to change. The fluctuation of CCI curve is because of the color distort during the image enhancement. The curve of CNI fluctuant ascends with the increase of the defogging effect. When the image achieves the best defogging effect, the value begins to decline. CNI stands for the naturalness of the image color. Since the image color may also be natural when there is a little fog, the curve has some peaks after the image achieves the best defogging effects. Thus, the most natural image does not necessarily have the best clearness effect, but the image with a good defogging effect must have high CNI value.

5.2 Construction of comprehensive evaluation function

In practice, one usually requires a single overall defogging effect measure of the entire image. Thus, three components are combined to yield an overall defogging effect measure:

$$\mathrm{CNC}(x, y) = f(e(x, y), \mathrm{CNI}(y), \mathrm{CCI}(y)) \tag{12}$$

For the overall variation trend of the three indexes shown in Fig. 10, it is noted that the peak of CNI curve stands for the most natural result, but it is not necessarily the best defogging effect. However, the best effect must have good naturalness (high CNI value). When the image is over-enhanced, the color is distorted, and CNI goes down rapidly. For e and CCI, they achieve the best effect before reaching their peaks. When the image is over-enhanced, the curves continue ascending. After reaching their peaks, these curves just begin to go down. Therefore, if the uptrend of e and CCI (from their best effect points to their curve's peaks) can be largely counteracted by the downtrend of CNI, the peak of CNC curve can be more close to the real best effect point. Meanwhile, the value change of CNI is small, while that of e and CCI is relatively big. Thus, the effect of e and CCI on the CNC index needs to be weakened. The CNC index between image signals x and y can be defined as

$$\mathrm{CNC}(x, y) = e(x, y)^{1/n_1} \cdot \mathrm{CNI}(y) + \mathrm{CCI}(y)^{1/n_2} \cdot \mathrm{CNI}(y) \tag{13}$$

where $n_1 \geq 1$ and $n_2 \geq 1$ are parameters used to weaken the variation trend of e and CCI. When n_1 or n_2 is small, the maximum value is achieved for the over-enhanced image. With the two values increasing, the values of $e(x, y)^{1/n_1} \cdot \mathrm{CNI}(y)$ and $\mathrm{CCI}(y)^{1/n_2} \cdot \mathrm{CNI}(y)$ tend to be stable, and the peaks of their curve move to the left (the best effect point). Since the CNC index is the sum of the two terms, it has the similar trend, as shown in Fig. 11. Therefore, choosing suitable n_1 and n_2 can make CNC index stable and ensure that the curve peak is close to the best defogging effect as much as possible. n_1 and n_2 are application-based. When fixing $n_1 = n_2 = 5$ in this experiment, the value can keep the performance of $e(x, y)^{1/n_1} \cdot \mathrm{CNI}(y)$ and $\mathrm{CCI}(y)^{1/n_2} \cdot \mathrm{CNI}(y)$ stable. Thus, the larger the value of CNC is, the better the defogging effect will be.

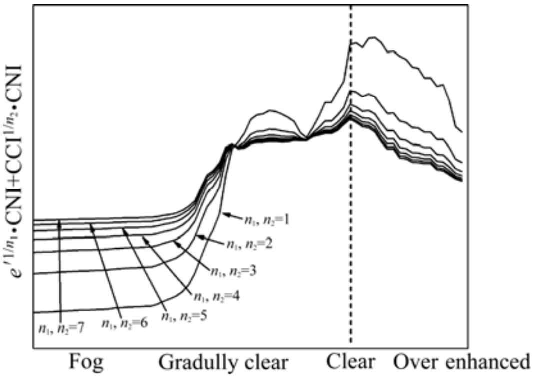

Fig. 11 Overall variation trend curve of CNC by tuning n_1 and n_2

5.3 Application example

5.3.1 Dynamically adjust algorithm parameter

CNC index is used for dynamically adjusting the algorithm parameter. Therefore, resorting to feed-back mechanism, the static open-loop parameter estimation issue can be transformed into the dynamical close-loop parameter adjustment. The following are two illustrative examples.

In HE's method [3], the parameter ω alters the amount of haze at all depths. If ω is adjusted downward, more haze will be kept, and vice versa. The ω was suggested to be 0.95 by the author. The value can keep a slight amount of haze effect around at all depths. However, ω sometimes needs to be decreased when an image contains substantial sky regions, otherwise the sky region may wind up having artifacts. An example indicating the need to decrease ω is shown in Fig. 12. Figure 12(b) is with ω=0.95. As can be seen, the sky looks contoured since the haze removed by HE's approach is too strong in this region. With ω=0.12 automatically set by CNC in Fig. 12(c), the sky region becomes brighter and smoother, which looks more natural.

The parameter p in TAREL's algorithm [2] was used to control the aspect of the visibility restoration, and was set between 90% and 98%. This means that 90% or 98% of the amount of atmospheric veil is removed. This parameter is useful to compromise between highly restored visibility (when p is closed to 1) where colors may appear over saturated and too dark, and less restored visibility where colors are less saturated and thus clearer. Thus, a proper p value should be determined. As can be seen in Fig. 13, the restored images look more pleasing with p=0.96 automatically set by CNC, which basically conforms to p=0.95 set by TAREL.

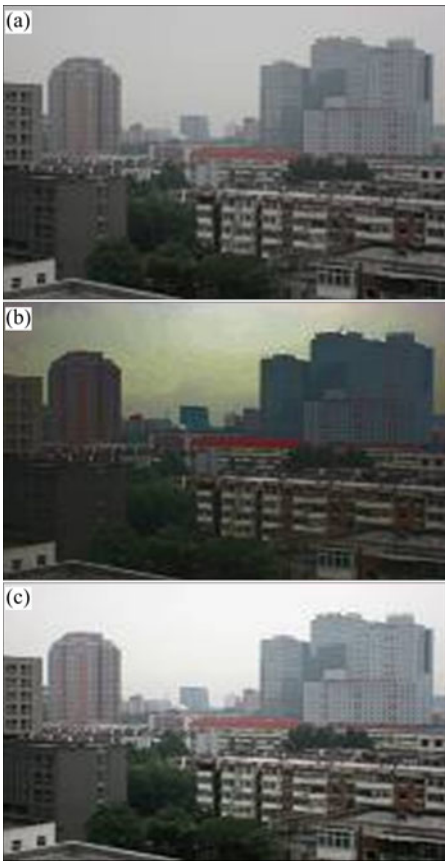

Fig. 12 Original image (a), unpleasing contour effect with ω= 0.95 (b) and smoother sky region using ω=0.12

5.3.2 Objective evaluation for color image

As mentioned above, the best defogging images for Figs. 5−7 are Fig. 5(c), Fig. 6(c) and Fig. 7(d). This can be verified by the proposed index CNC in Table 3. Good results are described by high value of CNC. From Table 3, it is seen that the highest values of CNC are 1.16 (TAN's method), 1.396 (TAREL's method) and 1.95 (HE's method). This confirms our observations in Figs. 5−7 and indicates that our proposed index delivers better consistency with human visual perception for color images. Notice that the CNC value cannot be obtained for gray level image since there are no color information for CNI and CCI computation. Furthermore, the conclusions drawn by using the assessment method based on visibility edges are inconsistent with the CNC results. From Table 4, it is deduced that the values of e and $\bar{r}$ for TAREL's method are generally greater than those of HE's method, which means the defogging effect is better. However, compared with HE's method, TAN's results have the apparent problems of over-enhancement and color distortion. Thus, the results of existing assessment method do not conform to the human visual perception.

6 Experimental comparison and analysis

To validate the effectiveness of the three proposed

Fig. 13 Haze removal results with different p values: (a) Original image; (b) Haze removal result with p=0.7; (c) Haze removal result with p=0.99; (d) More pleasing result with p=0.96

Table 3 CNC index computed for three compared methods

Image No.	TAN's method	TAREL's method	HE's method
Fig. 5	1.13	1.16	1.06
Fig. 6	0.94	1.39	1.26
Fig. 7	1.49	1.21	1.95

assessment methods and the simulated fog generation method, experiments were performed with the actual color and gray level images. An illustrative example is shown in Fig. 14. Figure 14(a) shows the actual fog free image, and its corresponding foggy image is shown in Fig.14(c). Figure 14(b) shows the simulated foggy image. Figures 14(d) and (e) are respectively the defogging results of TAREL's and HE's methods for simulated foggy image (Fig. 14(b)). Figures 14(f) and (g) are the defogging results for actual foggy image (Fig. 14(c)). One can notice that the result of HE's method seems more natural than TAREL's result. The statistics of AD, f and CNC in Table 5 also confirm this conclusion. Table 6 gives a comparison of the four assessment methods mentioned in this work.

The assessment index is tested on more sample natural color images (300 test images), which consists of foggy image from internet database and real scene captured by Canon S80 with different scene, weather and fog density. Figure 15(a) shows the statistical result of AD for 150 images, and Fig. 15(b) shows the CNC result

Table 4 Results of contrast enhancement assessment methods

Image No.	TAN's method			TAREL's method			HE's method		
	e	$\bar{r}$	σ/%	e	$\bar{r}$	σ/%	e	$\bar{r}$	σ/%
Fig. 5	10.2390	2.7029	0	10.2197	3.8801	0	6.5036	1.2876	0.0139
Fig. 6	0.6862	2.8696	0.4954	0.7392	3.0083	0.0013	0.3442	1.2023	1.5952
Fig. 7	0.5322	3.1269	0.8492	0.7850	2.0673	0	0.6589	1.6112	0.2071
Fig. 8	0.4376	2.8568	0.3188	0.3449	4.0245	5.7546	0.3595	1.8335	2.2815

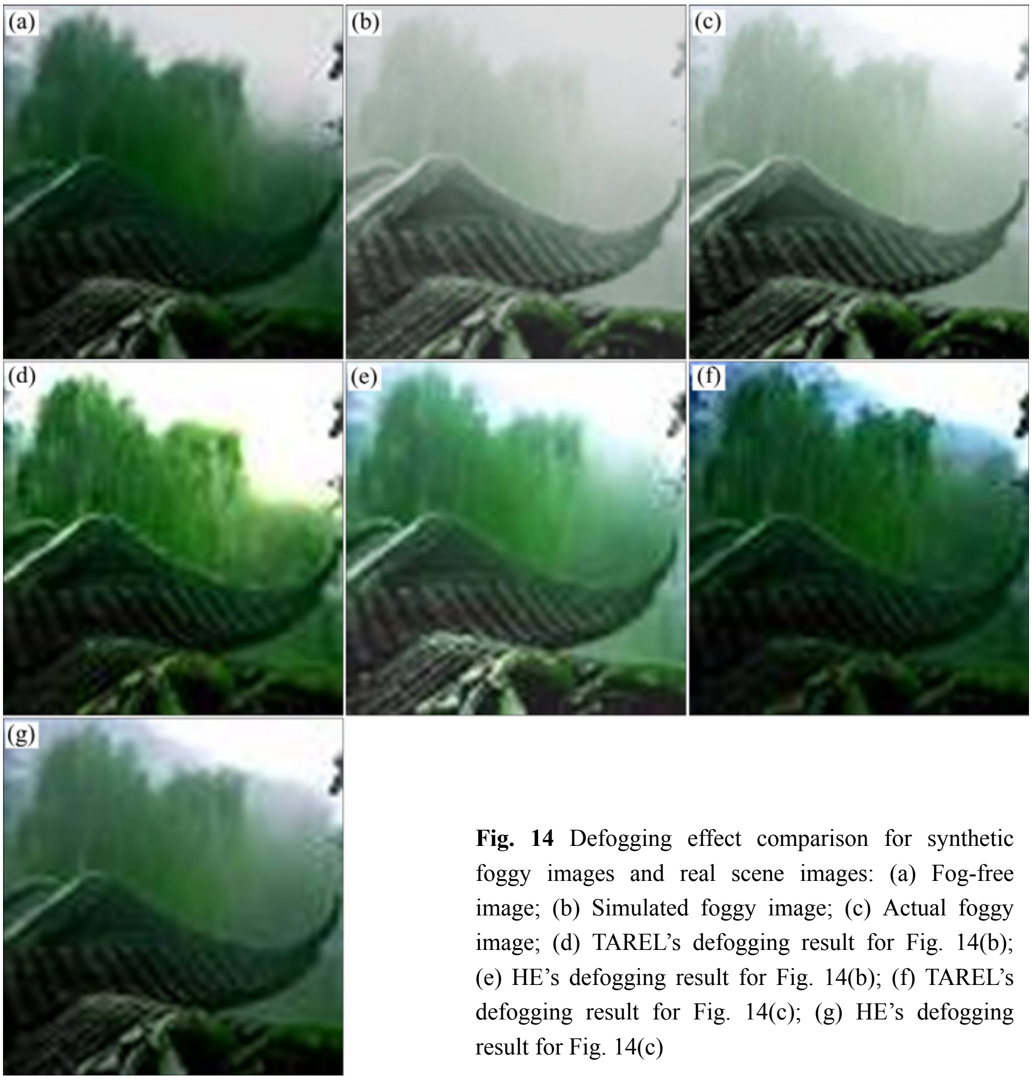

Fig. 14 Defogging effect comparison for synthetic foggy images and real scene images: (a) Fog-free image; (b) Simulated foggy image; (c) Actual foggy image; (d) TAREL's defogging result for Fig. 14(b); (e) HE's defogging result for Fig. 14(b); (f) TAREL's defogging result for Fig. 14(c); (g) HE's defogging result for Fig. 14(c)

Table 5 Index computed for two compared algorithms by using proposed assessment methods

Index	Simulated fog			Actual fog	
	Nothing	TAREL's method	HE's method	TAREL's method	HE's method
AD	73.01	45.75	22.94	20.08	15.92
f	0.0769	0.0312	0.0461	0.0255	0.0131
CNC	—	2.52	2.74	2.59	2.78

Table 6 Comparison of four assessment methods

Method	Category	Applicable object	Method feature
Visibility edge method	No-reference	Color and gray level image	Assess from image contrast
Synthetic image method	Full-reference	Color and gray level image	Resort to synthetic reference image
Fog density method	No-reference	Gray level image	Using fog veil and dark channel to estimate density
Human visual perception method	No-reference	Color image	Assess from both contrast and color quality

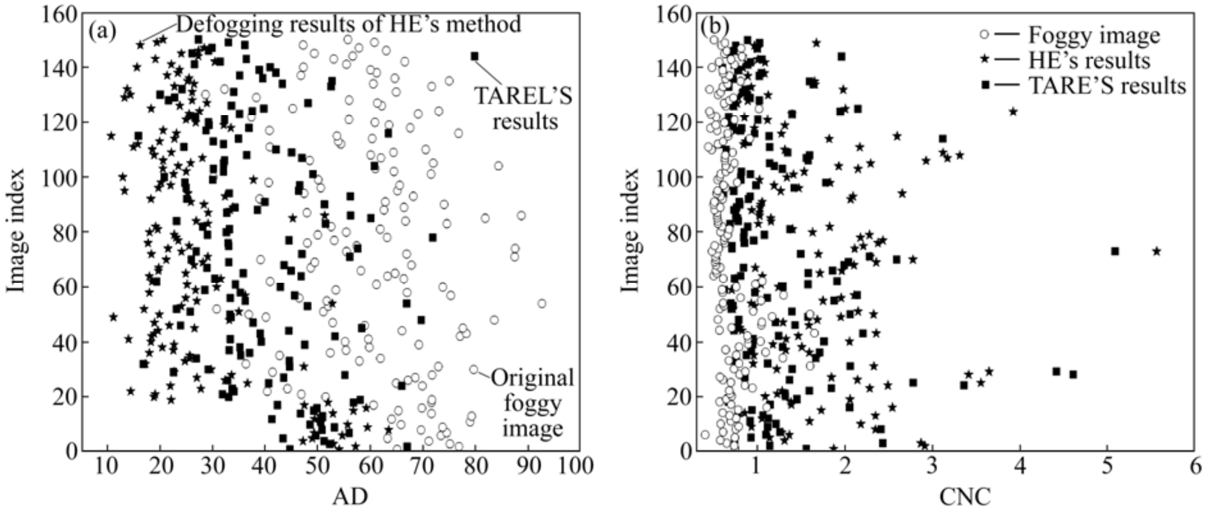

Fig. 15 Index statistical results for test images: (a) AD; (b) CNC

for other 150 images. The horizontal axes are the assessment index values and vertical axes are the image number index. From Fig. 15(a), it is seen that the AD of HE's method is smaller than that of TAREL's method. The smaller the value of AD is, the better the defogging effect will be. Thus, the conclusion that HE's method has better clearness effect can be drawn. For Fig. 15(b), it is clear that the CNC of original foggy image is clustered between 0 and 2, while the CNC of TAREL's and HE's results are distributed between 0.5 and 5.5, 0.5 and 6, respectively. The higher the value of CNC is, the better the defogging effect will be. Thus, it is deduced that the visual effect of original image can be effectively improved by using the two defogging algorithms, and one can notice that the overall value of CNC of HE's method is a little greater than that of TAREL's method. This indicates that, on the whole, HE's defogging effect is slightly better for this image test database, which is consistent with the assessment results of AD and human visual perception.

7 Conclusions

1) The limitation of the existing assessment method is enumerated, and three assessment methods are proposed aiming at assessing image defogging algorithm. One is using synthetic foggy image as reference image to assess defogging algorithm. The other two are computing the fog density for gray level image or constructing assessment system for color image from human visual perception to assess defogging algorithm without reference image. The results of a variety of test images show the effectiveness and reliability of the proposed methods.

2) The CNC index is used to dynamically adjust the algorithm parameter. However, only two defogging algorithms are considered here. In the future, feed-back mechanism will be resorted to transform the static open-loop parameter estimation issue into the dynamical close-loop parameter adjustment for more defogging

algorithms.

Acknowledgment

The authors would like to thank Erik Matlin and Kaelan Yee for providing HE's source code, Dr. Jean-Philippe Tarel and Dr. Nicolas Hautiere for providing the matlab code of their approach, and Dr. Tan for providing his defogging image.

References

[1] TAN R T. Visibility in bad weather from a single image [C]// Proceedings of the IEEE Conference on Computer Vision and Pattern Recognition. Anchorgae, USA: IEEE Engineering Society, 2008: 1−8.

[2] TAREL J P, HAUTIERE N. Fast visibility restoration from a single color or gray level image [C]// Proceedings of the 12th IEEE International Conference on Computer Vision. Kyoto, Japan: IEEE Engineering Society, 2009: 2201−2208.

[3] HE Kai-ming, SUN Jian, TANG Xiao-ou. Single image haze removal using dark channel prior [C]// Proceedings of the IEEE Conference on Computer Vision and Pattern Recognition. New York, USA: IEEE Society, 2009: 1956−1963

[4] WANG Z, BOVIK A C, SHEIKH H R, SIMONCELLI E P. Image quality assessment: From error visibility to structural similarity [J]. IEEE Trans Image Processing, 2004, 13(4): 600−612.

[5] ESKCIOGLU A M, FISHER P S. Image quality measures and their performance [J]. IEEE Trans Communication, 1995, 43(12): 2959−2965.

[6] WANG Zhou, SIMONCELLI E P. Reduced-reference image quality assessment using a wavelet-domain natural image statistic model [C]// Proceedings of SPIE's 17th Annual Symposium on Electronic Image. Washington: SPIE Digital Library, 2005: 17−20.

[7] CARNEC M, CALLET P L, BARBA D. Objective quality assessment of color images based on a generic perceptual reference [J]. Signal Processing: Image Communication, 2008, 23(4): 239−256.

[8] HAUTIERE N, TAREL J P, AUBERT D, DUMONT E. Blind contrast enhancement assessment by gradient ratioing at visible edges [J]. Image Analysis and Stereology Journal, 2006, 27(2): 87−95.

[9] YU Jing, XU Dong-bin, LIAO Qing-min. Image defogging: A survey [J]. Journal of Image and Graphics, 2011, 16(9): 1561−1576. (in Chinese)

[10] LI Da-peng, YU Jing, XIAO Chuang-bai. No-reference quality assessment method for defogged images [J]. Journal of Image and Graphics, 2011, 16(9): 1753−1757. (in Chinese)

[11] YAO Bo, HUANG Lei, LIU Chang-ping. Research on an objective method to compare the quality of defogged images [C]// Proceedings of Chinese Conference on Pattern Recognition. New York: IEEE Society, 2009: 1−5. (in Chinese)

[12] BLACKWELL H R, BLACKWELL O M, BODMANN H W. An analytic model for describing the influence of lighting parameters upon visual performance. CIE Report 19.2 [R]. Vienna: Central Burean of the International Commission on Illumination (CIE) [R], 1981.

[13] ADRIAN W D I. Visibility of targets: Model for calculation [J]. Lighting Research and Technology, 1989, 21(4): 181−188.

[14] NAYAR S K, NARASIMHAN S G. Vision in bad weather [C]// Proceedings of the IEEE International Conference on Computer Vision. New York: IEEE Engineering Society, 2002: 820−827.

[15] YU Jing, LI Dang-peng, LIAO Qing-min. Physics-based fast single image fog removal [J]. Acta Automatics Sinica, 2011, 37(2): 143−149. (in Chinese)

[16] ROSSUM Z, NIEUWENHUIZN T. Multiple scattering of classical waves: Microscopy, mesoscopy and diffusion [J]. Reviews of Modern Physics, 1999, 71(1): 313−371.

[17] YENDRIKHOVSKIJ S, BLOMMAERT F, RIDDER H D. Perceptual optimal color reproduction [C]// Proceedings of SPIE. Washington, USA: SPIE Digital Library, 1998: 274−281.

[18] HUANG Kai-qi, WANG Qiao, WU Zhen-yang. Natural color image enhancement and evaluation algorithm based on human visual system [J]. Computer Vision and Image Understanding, 2006, 103(1): 52−63.

(Edited by FANG Jing-hua)